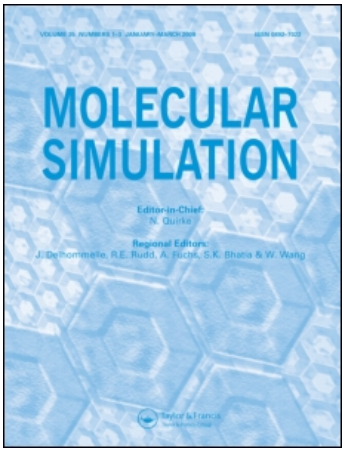

Molecular Simulation
Publication details, including instructions for authors and subscription information:
http://www.informaworld.com/smpp/title~content=t713644482

Static Dielectric Constant of the Polarizable Stockmayer Fluid. Comparison of the Lattice Summation and Reaction Field Methods

Claude Millot[a]; Jean-Christophe Soetens[a]; Marília T. C. Martins Costa[a]
[a] Laboratoire de chimie théorique, URA CNRS n° 510, Boulevard des Aiguillettes, BP 239, Vandoeuvre-lès-Nancy Cedex, France

To cite this Article Millot, Claude , Soetens, Jean-Christophe and Costa, Marília T. C. Martins(1997) 'Static Dielectric Constant of the Polarizable Stockmayer Fluid. Comparison of the Lattice Summation and Reaction Field Methods', Molecular Simulation, 18: 6, 367 — 383
To link to this Article: DOI: 10.1080/08927029708024131
URL: http://dx.doi.org/10.1080/08927029708024131

Molecular Simulation, 1997, Vol. 18, pp. 367–383
Reprints available directly from the publisher
Photocopying permitted by license only

STATIC DIELECTRIC CONSTANT OF THE POLARIZABLE STOCKMAYER FLUID. COMPARISON OF THE LATTICE SUMMATION AND REACTION FIELD METHODS

CLAUDE MILLOT, JEAN-CHRISTOPHE SOETENS and MARÍLIA T. C. MARTINS COSTA

Laboratoire de chimie théorique, URA CNRS n° 510,
Boulevard des Aiguillettes, BP 239, 54506
Vandoeuvre-lès-Nancy Cedex, France

(Received February 1996; accepted August 1996)

The static dielectric constant of the polarizable Stockmayer fluid is computed through Molecular Dynamics simulations where long range electrostatic interactions are computed either by reaction field or by lattice summation method (Ladd expansion). The effects on the simulated dielectric constant of the truncation of the Ladd expansion and of the cutoff distance in reaction field geometry have been explored for different values of the polarizability.

Keywords: Molecular Dynamics simulation; polarizable Stockmayer fluid; dielectric constant; lattice summation; reaction field method

1. INTRODUCTION

The computation of the static dielectric constant of polar fluids has received a great deal of attention in the last two decades in theoretical works [1–6] as well as in computer simulations [7]. Most of the simulation studies have focused on simple models, as the Stockmayer fluid [8–11], the dipolar soft sphere [12–14] and hard sphere fluids [4] and a number of molecular liquids, mainly water models [15–21]. In the field of Monte Carlo (MC) and Molecular Dynamics (MD) simulations, much effort has been devoted to the methodological aspects of such calculations [4, 7, 8, 22–26]. The notorious

difficulty of obtaining this fundamental physical property with reasonable accuracy (implying very long simulations) has motivated some work aiming to improve the efficiency of the simulation. In particular, it has been shown that the reaction field technique can lead to a static dielectric constant of the Stockmayer fluid in good agreement with the lattice sum prediction [27, 10]. Moreover, Neumann has studied the sensitivity of the result to the truncation of the Ladd expansion [28, 29] and shown that a truncation at the order 6 already gives a result close to the converged result [10]. Due to the large amount of computer time required, the dielectric constant of polarizable fluids have been less studied. The pioneering work of Pollock, Alder and Patey [30] on the polarizable Stockmayer fluid has shown that the electronic polarizability has a considerable effect on the dielectric constant. Mooij *et al.* [31] have reported simulation results of the static dielectric constant of mixtures of Stockmayer and polarizable Lennard-Jones particles. The dielectric constant of water has also been determined using polarizable models [32–35]. With the appearance of parallel computers, molecular modelling including explicitly the polarizability in the force field is rapidly developing and computations of the dielectric properties of polarizable fluids will soon become routine.

In this work we are interested in comparing the static dielectric constant of the polarizable Stockmayer fluid obtained from MD simulations where long range electrostatic interactions are computed either by a lattice summation technique (Ladd summation supplemented by a conducting boundary reaction field) or by a Barker-Watts reaction field approach [36]. Several MD simulations have been carried out with different values of the polarizability, number of particles, truncation of the Ladd expansion, and cutoff distance in reaction field geometry. Such comparisons supplement similar studies done with the (non-polarizable) Stockmayer fluid [10].

The system studied and the details of the computations are described in section II. Our results for thermodynamical, dynamical and dielectric properties are presented and discussed in section III.

2. METHOD AND COMPUTATIONAL DETAILS

The total potential energy of N polar/polarizable Stockmayer particles can be written [37]:

$$U = U_{LJ} + U_{dip} + U_{cr} = \frac{1}{2}\sum_i \sum_{j \neq i} 4\varepsilon_{LJ}\left(\left(\frac{\sigma_{LJ}}{r_{ij}}\right)^{12} - \left(\frac{\sigma_{LJ}}{r_{ij}}\right)^{6}\right)$$

$$+\frac{1}{2}\sum_i\sum_{j\neq i}(\boldsymbol{\mu}_i+\mathbf{p}_i)\mathbf{T}_{ij}(\boldsymbol{\mu}_j+\mathbf{p}_j)+\frac{1}{2}\sum_i\frac{\mathbf{p}_i^2}{\alpha} \tag{1}$$

where $\boldsymbol{\mu}_i$ and $\mathbf{p}_i$ are the permanent and induced dipole moments respectively, r_{ij} the distance between particle i and j, α the point isotropic polarizability and $\mathbf{T}_{ij}$ is the dipolar interaction tensor. U_{LJ} is the Lennard-Jones energy, U_{dip} is the total dipole-dipole electrostatic energy of the system and U_{cr} the reversible work required to create the induced dipoles.

The induced moments are obtained from the equation:

$$\mathbf{p}_i=-\sum_{j\neq i}\alpha\mathbf{T}_{ij}(\boldsymbol{\mu}_j+\mathbf{p}_j) \tag{2}$$

The induced moments are computed in an iterative manner. In our program, they are initiated with the values of the previous MD step and convergence is achieved in 5–7 iterations. Inserting Eq. (2) in the expression of U_{cr} of Eq. (1) leads to:

$$U_{\mathrm{dip}}+U_{\mathrm{cr}}=U_{\mathrm{es}}+U_{\mathrm{ind}}=\frac{1}{2}\sum_i\sum_{j\neq i}\boldsymbol{\mu}_i\mathbf{T}_{ij}\boldsymbol{\mu}_j+\frac{1}{2}\sum_i\sum_{j\neq i}\mathbf{p}_i\mathbf{T}_{ij}\boldsymbol{\mu}_j \tag{3}$$

U_{es} (interactions between permanent dipoles) and U_{ind} (interactions between induced and permanent dipoles) are respectively called *electrostatic energy* and *induction energy* in the theory of intermolecular interactions.

In reaction field geometry, the electrostatic tensor is given by:

$$\mathbf{T}_{ij}=\left(\frac{\mathbf{1}}{r_{ij}^3}-\frac{3\mathbf{r}_{ij}\mathbf{r}_{ij}}{r_{ij}^5}\right)-\frac{2(\varepsilon_{RF}-1)}{2\varepsilon_{RF}+1}\frac{\mathbf{1}}{R_{\mathrm{c}}^3} \tag{4}$$

if the distance between both particles r_{ij} is smaller than R_{c} (cutoff radius), ε_{RF} is the dielectric constant of the continuum and $\mathbf{1}$ the 3×3 unit matrix. If $r_{ij}>R_{\mathrm{c}}$, $\mathbf{T}_{ij}$ is zero.

The Ladd approach [28,29] is a systematic expansion of the lattice sums leading, in the case of a cubic box, to a simple expression for the interaction tensor:

$$\mathbf{T}_{ij}=\left(\frac{\mathbf{1}}{r_{ij}^3}-\frac{3\mathbf{r}_{ij}\mathbf{r}_{ij}}{r_{ij}^5}\right)-\frac{2(\varepsilon_{RF}-1)}{2\varepsilon_{RF}+1}\frac{4\pi}{3V}\mathbf{1}+\mathbf{T}_4+\mathbf{T}_6+\mathbf{T}_8+\mathbf{T}_{10}+\cdots \tag{5}$$

where the second term is a reaction field contribution, V is the volume of the cubic simulation cell and the elements of the tensors $\mathbf{T}_n$ are polynomials of cubic symmetry; their expressions up to $\mathbf{T}_{10}$ have been given by Neumann [10]. Note that i) Neumann defines the interaction energy between two dipole moments as $-\boldsymbol{\mu}_i \mathbf{T}_{ij} \boldsymbol{\mu}_j$, and we use $\boldsymbol{\mu}_i \mathbf{T}_{ij} \boldsymbol{\mu}_j$ and ii) we give electrostatic formulae in the e.s.u. system.

In Eqs (1)–(5), the self interaction terms (corresponding to the interaction of each particle with its own reaction field) are neglected. This point is discussed in Appendix A.

The choice $\varepsilon_{RF} = \infty$ insures that the Ladd summation is formally equivalent to the usual Ewald summation technique [10]. In this work, the value $\varepsilon_{RF} = \infty$ has been chosen in reaction field geometry (RF) and in lattice summation geometry (LS). The Ladd expansion is truncated after the $\mathbf{T}_6$, $\mathbf{T}_8$ or $\mathbf{T}_{10}$ terms (LS6, LS8 and LS10 respectively). The static dielectric constant ε_0 of the system is obtained from the fluctuation formula [30]:

$$\frac{\varepsilon_0 - 1}{3} = \frac{4\pi}{9VkT} \langle \mathbf{M}^2 \rangle + \frac{\varepsilon_\infty - 1}{3} \tag{6}$$

where V is the cell volume, $\mathbf{M}$ the total dipole moment (permanent + induced) of the simulation cell and ε_∞ the high-frequency dielectric constant, estimated from the Clausius-Mossotti relationship:

$$\frac{\varepsilon_\infty - 1}{\varepsilon_\infty + 2} = \frac{4\pi}{3} \rho\alpha \tag{7}$$

where ρ is the particle density and α the point polarizability. Pollock *et al.* [30] have shown that Eq. (6) is valid in the usual Ewald summation geometry ($\varepsilon_{RF} = \infty$); they have also given the formula

$$\frac{\varepsilon_0 - 1}{\varepsilon_0 + 2} = \frac{4\pi}{9VkT} \langle \mathbf{M}^2 \rangle + \frac{\varepsilon_\infty - 1}{\varepsilon_\infty + 2} \tag{8}$$

for the case of a sphere in vacuum ($\varepsilon_{RF} = 1$) and the equation

$$\frac{(\varepsilon_0 - 1)(2\varepsilon_0 + 1)}{9\varepsilon_0} = \frac{4\pi}{9VkT} \langle \mathbf{M}^2 \rangle + \frac{(\varepsilon_\infty - 1)(2\varepsilon_\infty + 1)}{9\varepsilon_\infty} \tag{9}$$

for the case of a sphere embedded in an infinite medium with its own dielectric constant ($\varepsilon_{RF} = \varepsilon_0$). In Appendix B, it is shown that Eq. (6) is also

valid in RF geometry when $\varepsilon_{RF} = \infty$. For the non polarizable case, Eq. (6) (with $\mathbf{M} = \sum_i \boldsymbol{\mu}_i$ and $\varepsilon_\infty = 1$) is valid for both RF and lattice summation geometry if $\varepsilon_{RF} = \infty$ [23]. In Eq. (6), (8) and (9), it is assumed that the system is isotropic and that $\langle \mathbf{M} \rangle = 0$. When $\langle \mathbf{M} \rangle \neq 0$, $\langle \mathbf{M}^2 \rangle$ has to be replaced by $\langle \mathbf{M}^2 \rangle - \langle \mathbf{M} \rangle^2$ in the fluctuation formulae; as extremely long simulations are required to get $\langle \mathbf{M} \rangle = 0$, in practice $\langle \mathbf{M} \rangle$ is monitored during the simulation and used to obtain ε_0.

MD simulations are done in NEV ensemble, with a time step $\Delta t = 3$ fs for a number of particles ranging from $N = 125$ to $N = 729$. The equations of motions of the particles, considered as linear molecules, are integrated using an algorithm due to Fincham [38]. The cutoff radius is taken to be equal to half the cell edge in RF geometry. In LS geometry, the short range Lennard-Jones interactions are also truncated at half the cell edge; in that way, the RF and LS models differ only by the treatment of the electrostatic interactions. Because of the use of a cutoff, the energy is not exactly conserved and velocities are rescaled every 100 time steps in order to maintain the temperature close to 300 K and to avoid energy drift. Between two rescalings, the drift in total energy (more severe in RF than in LS geometry) is less than 1% for $N = 256$ and $\alpha^* = \alpha/\sigma_{LJ}^3 = 0.05$ in RF geometry.

The calculations have been done on IBM RISC/6000 workstations and with a parallel version of our program on an IBM SP1 computer. With $N = 256$, one LS10 and RF time step costs 7.2 s and 3.0 s respectively on one SP1 processor. Using eight processors, the waiting time has been divided by 7.3 in LS10 geometry and 6.4 in RF geometry.

As a starting point, a state point of the Stockmayer fluid well studied in computer simulation has been chosen: $\rho^* = N\sigma_{LJ}^3/V = 0.822$, $T^* = kT/\varepsilon_{LJ} = 1.15$ and $\mu^{*2} = \mu^2/(kT\sigma_{LJ}^3) = 3.0$. MD simulations have been done with different values of the polarizability $\alpha^* = 0.025$, 0.05 and 0.075. With these values of the polarizability, ε_∞ is equal to 1.3, 1.6 and 2.0 respectively; consequently the term $(\varepsilon_\infty - 1)/3$ in Eq. (6) is numerically very small in all our simulations of highly polar/polarizable systems. The nonpolarizable model has also been reexamined, our results are in agreement with the results of Neumann [10]. Thermodynamic properties of the polarizable Stockmayer fluid in a large range of state points have been investigated by Kriebel and Winkelmann [39]. The parameters of the simulations in real and reduced units are given in Table I.

TABLE I MD simulation parameters of the polarizable Stockmayer fluid (in real and reduced units)

ε_{LJ}/kcal.mol^{-1}	0.518
σ_{LJ}/Å	2.906
$\rho^* = \rho\sigma_{LJ}^3$	0.822
T/K	300
$T^* = kT/\varepsilon_{LJ}$	1.15
μ/D	1.6273
$(\mu^*)^2 = \mu^2/(kT\sigma_{LJ}^3)$	3.00
α/Å^3	1.2271
$\alpha^* = \alpha/\sigma_{LJ}^3$	0.05
m/g.mol^{-1}	40.0
$I_{xx} = I_{yy}$/g.mol^{-1}.Å^2	8.445
Δt/ps	0.003
$\Delta t^* = \Delta t(\varepsilon_{LJ}/m\sigma_{LJ}^2)^{1/2}$	0.0024

3. RESULTS AND DISCUSSION

Some thermodynamic properties are given in Table II. The results for the static dielectric constant and related quantities are given in Figure 1 and Table III.

For the system with $\alpha^* = 0.025$ and $N = 256$, it is shown that the Ladd expansion converges quite quickly, LS8 and LS10 give roughly the same result, differing by a few percent from the LS6 value. Our estimate for ε_0 at this state point is 130 ± 12. The RF geometry provides an estimate (125 ± 10) in good agreement with the value.

When the polarizability increases to the value $\alpha^* = 0.05$, keeping $N = 256$, the situation is significantly different. The Ladd expansion converges more slowly, LS6 leads to a mere 75% of the LS10 estimation for ε_0. RF and

TABLE II Thermodynamic properties of the polarizable Stockmayer fluid ($\mu^{*2} = 3.0, T^* = 1.15, \rho^* = 0.822$) as a function of reduced polarizability $\alpha^*(U^* = U/N\varepsilon_{LJ}; P^* = P\sigma_{LJ}^3/\varepsilon_{LJ})$

α^*	N		U^*	U^*_{kin}	U^*_{es}	U^*_{ind}	U^*_{LJ}	T/K	P^*
0.025	256	LS6	−10.62	2.88	−4.97	−0.61	−5.04	300.5	−0.20
		LS8	−10.61	2.89	−4.96	−0.61	−5.04	301.1	−0.25
		LS10	−10.60	2.88	−4.95	−0.61	−5.04	300.5	−0.26
		RF	−10.55	2.92	−4.91	−0.60	−5.05	303.8	−0.22
0.05	256	LS6	−11.73	2.88	−5.40	−1.60	−4.74	300.7	−0.37
		LS8	−11.72	2.89	−5.39	−1.60	−4.73	301.6	−0.31
		LS10	−11.72	2.92	−5.40	−1.60	−4.71	300.5	−0.29
		RF	−11.56	2.93	−5.28	−1.53	−4.74	300.6	−0.47
0.075	256	LS10	−15.04	2.89	−6.85	−4.64	−3.55	300.0	5.13
		RF	−13.65	2.93	−6.24	−3.78	−3.62	305.4	1.91

TABLE III Dielectric properties of the polarizable Stockmayer fluid ($\mu^{*2} = 3.0, T^* = 1.15$, $\rho^* = 0.822$) as a function of reduced polarizability α^*. For sufficiently long runs, errors bars on ε_0 (given between parenthesis) are obtained from subaverages. $\langle M^{*2}\rangle, \langle M_x^*\rangle, \langle M_y^*\rangle, \langle M_z^*\rangle$: averages of the square and components of the total dipole moment of the simulation cell (reduced units). $\langle \mu_{tot}^{*2}\rangle$: average of the square of the total individual dipole (reduced units)

α^*	N		steps	$\langle M^{*2}\rangle$	$\langle M_x^*\rangle$	$\langle M_y^*\rangle$	$\langle M_z^*\rangle$	ε_0	$\langle \mu_{tot}^{*2}\rangle$
0.0	256	LS6[a]	10^5					67	3.00
		LS8[a]	1.25×10^5					67	3.00
		LS10[a]	10^5					64	3.00
		RF[a]	5×10^4					65	3.00
0.025	256	LS6	3×10^5	10278	5.5	0.7	1.0	121(10)	3.59
		LS8	"	11212	4.4	11.6	4.5	131(15)	3.59
		LS10	"	11104	−0.7	1.5	1.9	130(12)	3.59
		RF	"	10782	0.0	3.2	15.4	125(10)	3.58
0.05	125	LS6	2×10^5	12560	−11.2	3.5	23.4	283(20)	4.60
		LS8	"	16647	−9.5	14.0	1.2	390(40)	4.60
		LS10	"	14690	−16.5	4.9	−12.0	340(20)	4.59
		RF	"	7309	−4.9	1.3	3.2	170(20)	4.50
0.05	256	LS6	3×10^5	32953	−29.5	−2.7	−4.0	374(25)	4.60
		LS8	"	42926	22.2	−3.7	−14.2	491(35)	4.60
		LS10	"	43288	−18.8	−7.3	36.6	488(30)	4.60
		RF	"	31571	6.8	1.5	17.8	358(30)	4.56
0.05	343	RF	10^5	49918	−4.2	3.1	−32.7	423	4.58
0.05	729	RF	5×10^4	153184	−54.0	6.1	78.7	588	4.59
0.075	256	LS10	2×10^5	351070	518.3	−224.6	194.9	—	7.61
		RF	2×10^5	187481	−24.1	192.2	60.9	—	6.90

[a]: results for the non polarizable case from Ref. [10].

LS10 also exhibit large discrepancies, the RF estimation ($\varepsilon_0 = 360$) being much smaller than the LS10 value ($\varepsilon_0 \approx 490$).

For $\alpha^* = 0.05$, some RF and LS simulations with different cutoff distances using different numbers of particles ($N = 125, 256, 343$ and 729) have been done. Four simulations (RF, LS6, LS8 and LS10) with $N = 125$ particles in the simulation box show that this system size is insufficient to obtain the best estimate $\varepsilon_0 \approx 490$. In that case, the LS8 and LS10 results are 20–30% smaller than when $N = 256$ and LS6 and RF results are still significantly smaller. Kusalik has shown that the value of the cutoff in RF simulation has an effect on the dielectric constant larger than the particle number [14]. In our simulations in RF geometry, a cutoff value equal to half the cube edge is used, so we do not attempt to separate the effects of the cutoff value and of the sample size. Nevertheless, it seems reasonable that the observations done by Kusalik for polar non polarizable fluids remain valid for the polarizable fluids. When the number of particles is increased from $N = 256$ to

$N = 343$, the prediction of RF geometry for ε_0 increases from 360 to 420 (for a run of 10^5 time steps or 300 ps). This trend seems to be confirmed by the result of the RF simulation of 5 10^4 time steps with $N = 729$ which gives a value $\varepsilon_0 \approx 590$. It is worth emphasizing that this last simulation is however too short to give an accurate estimate of the dielectric constant; there is no doubts that this result is not converged, but the computer time requirement being 3.4 larger than for LS10 with $N = 256$, the simulation has not been repeated.

In Figure 2, the average of the squared total individual dipole moment for $\alpha^* = 0.05$ in RF and LS10 simulations as a function of the number of particles (and cutoff distance in RF geometry) is presented. It is clearly found that this property is quite underestimated for the shortest cutoff distances. This fact plays an additional role in the systematic underestimation of the dielectric constant for the smallest cutoff distances. It can also be observed that RF geometry leads to a more pronounced dependence of ε_0 with the size of the system (or cutoff value) than LS geometry and this seems to be correlated to the underestimation of the averaged individual induced moment. From our results we suggest that a sample size/cutoff distance large enough to give a value of the averaged individual dipole independent of the system size should be a criterion to be satisfied in order to obtain a value of the dielectric constant also independent of the system size.

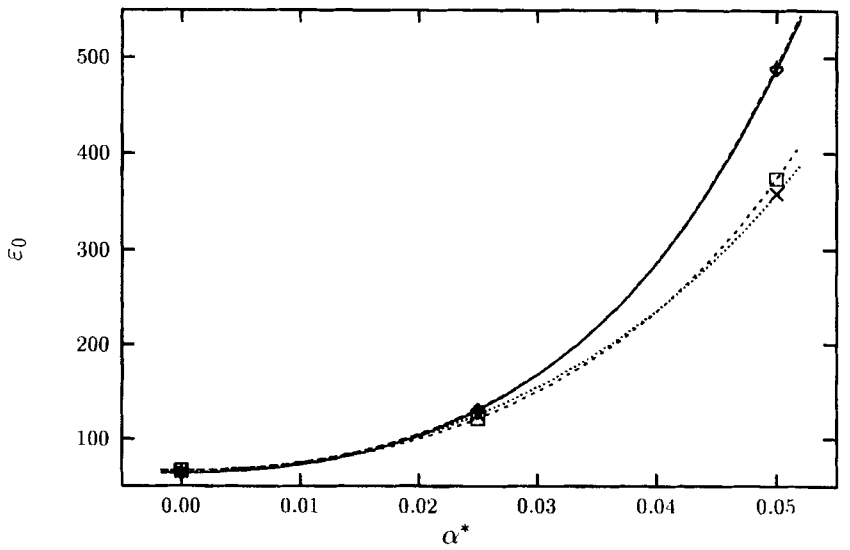

FIGURE 1 Static dielectric constant ε_0 of the polarizable Stockmayer fluid vs. reduced polarizability $\alpha^*(\mu^{*2} = 3.0, T^* = 1.15, \rho^* = 0.822, N = 256)$.
$\times$: RF; $\square$: LS6; $\diamond$: LS8; $+$: LS10. The curves are only a guide for the eye and do not result from a fitting procedure through the points (the same remark can be made for Figs. 2 and 3).

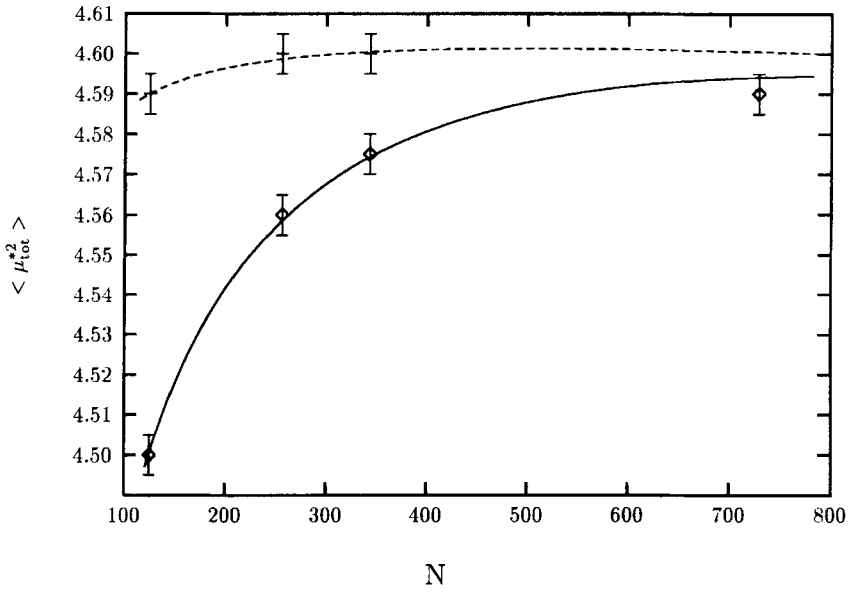

FIGURE 2 Average of the square of the total individual dipole moment of the polarizable Stockmayer fluid ($\mu^{*2} = 3.0, T^* = 1.15, \rho^* = 0.822, \alpha^* = 0.05$) vs. the number of particles N in the simulation box. The self interactions are neglected.
+: LS10; ◇: RF.

When the value of α^* increases, it is important to check if the system remains isotropic or if some kind of order is created. Some clues about the physical modifications arising in the system when α^* increases from 0.025 to 0.075 is given by the averages of the total dipole components in the laboratory referential $\langle M_x \rangle$, $\langle M_y \rangle$, $\langle M_z \rangle$, which should be equal to zero for an isotropic system. The more polarizable system has largest averaged values than the other ones, this is partly due to the shortness of the simulations but can also indicate the occurrence of electrostatic order. Existence of dipolar order is better probed by the computation of the order parameters $\langle P_1 \rangle$ and $\langle P_2 \rangle$ usual in the studies of nematics [40]. The instantaneous second-rank parameter P_2 is defined as the largest eigenvalue of the ordering matrix $\mathbf{Q}$ which elements are:

$$\mathbf{Q}_{\alpha\beta} = \frac{1}{N} \sum_{i=1}^{N} \frac{1}{2} (3u_i^{\alpha} u_i^{\beta} - \delta_{\alpha\beta}) \tag{10}$$

where u_i^α is the α component of the unit vector $\boldsymbol{\mu}_i$ along the dipole moment $\boldsymbol{\mu}_i$. The corresponding eigenvector is the instantaneous director $\mathbf{d}$ and the instantaneous first-rank order parameter P_1 is defined by:

$$P_1 = \frac{1}{N}\left|\sum_{i=1}^{N} \mathbf{u}_i.\mathbf{d}\right| \tag{11}$$

The dependence $\langle P_1 \rangle$ and $\langle P_2 \rangle$ for our system as a function of the polarizability is shown in Figure 3 and Table IV. They clearly indicate that for $\alpha^* = 0.025$, the system is isotropic (small departure from 0 for isotropic system is expected for finite size systems [41]) but when $\alpha^* = 0.05$, the system starts to exhibit a small electrostatic ordering in LS geometry. At $\alpha^* = 0.075$, the system is significantly ordered. The system being anisotropic, the dielectric constant is a tensor rather than a single number.

The dielectric relaxation time τ_D has been evaluated from the exponential decay of $\langle \mathbf{M}(0).\mathbf{M}(t) \rangle / \langle \mathbf{M}(0)^2 \rangle$. The values reported in Table V ($\tau_D^* = \tau_D \sqrt{\varepsilon_{LJ}/m\sigma_{LJ}^2}$ show that for $N = 256$ and $\alpha^* = 0.025$, LS10 and RF simulations are consistent; when α^* increases, differences start to be noticeable (though the error bar on τ_D is certainly large) when $\alpha^* = 0.05$ and increases

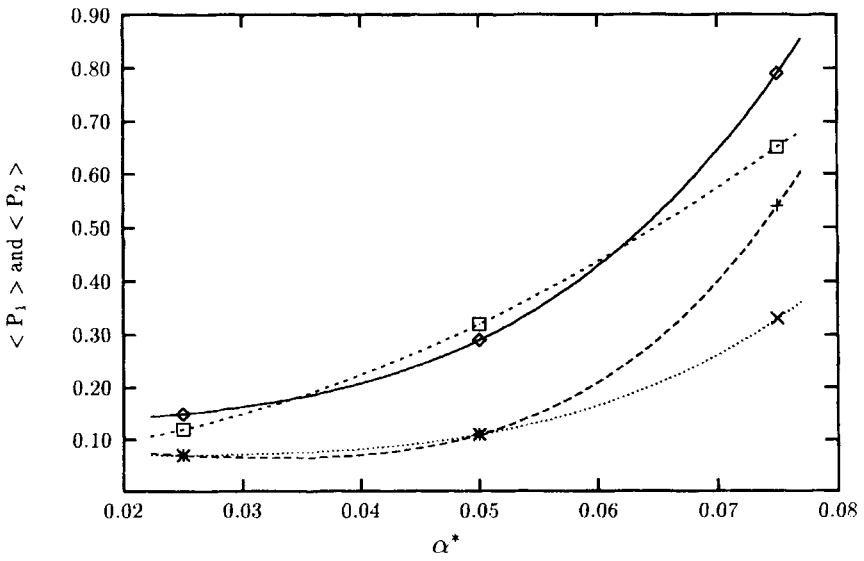

FIGURE 3 Orientational order parameters $\langle P_1 \rangle$ and $\langle P_2 \rangle$ for the polarizable Stockmayer fluid ($\mu^{*2} = 3.0$, $T^* = 1.15$, $\rho^* = 0.822$) vs. reduced polarizability α^*.
◇: $\langle P_1 \rangle$ and LS10; □: $\langle P_1 \rangle$ and RF; +: $\langle P_2 \rangle$ and LS10; ×: $\langle P_2 \rangle$ and RF.

TABLE IV Orientational order parameters ($\langle P_1 \rangle$ and $\langle P_2 \rangle$) as defined in the text for the polarizable Stockmayer fluid ($\mu^{*2} = 3.0, T^* = 1.15, \rho^* = 0.822$) for different values of the reduced polarizability α^* and simulation conditions

α^*	N		$\langle P_1 \rangle$	$\langle P_2 \rangle$
0.05	125	LS10	0.41	0.18
		RF	0.24	0.11
0.025	256	LS10	0.15	0.07
		RF	0.12	0.07
0.05	256	LS10	0.29	0.11
		RF	0.32	0.11
0.075	256	LS10	0.79	0.54
		RF	0.65	0.33

TABLE V Dynamical properties (reduced units) of the polarizable Stockmayer fluid ($\mu^{*2} = 3.0, T^* = 1.15, \rho^* = 0.822, N = 256$) for different values of the reduced polarizability α^*. D^*: translational diffusion coefficient; τ_1^* and τ_2^*: reorientational correlation times of the unit vector along the direction of the permanent dipole moment; τ_D^* and τ_μ^*: relaxation time of the autocorrelation function of the macroscopic and individual total (permanent + induced) dipole moment

α^*	0.025		0.05		0.075	
	LS10	*RF*	*LS10*	*RF*	*LS10*	*RF*
D^*	0.078	0.076	0.081	0.081	0.046	0.079
τ_1^*(a)	0.40[0.01]	0.38[0.00]	0.39[0.23]	0.46[0.06]	0.42[0.60]	0.60[0.13]
(b)	0.41[0.01]	0.38[0.00]	0.42[0.14]	0.47[0.05]	0.57[0.61]	0.59[0.39]
τ_2^*(a)	0.10[0.00]	0.10[0.00]	0.14[0.02]	0.16[0.00]	0.18[0.23]	0.28[0.07]
(b)	0.10[0.00]	0.10[0.00]	0.13[0.02]	0.16[0.00]	0.18[0.31]	0.33[0.08]
τ_D^*	2.2	2.0	9.3	6.6	> 500	50
τ_μ^*	0.40[0.01]	0.40[0.00]	0.55[0.13]	0.51[0.07]	0.57[0.71]	0.66[0.42]

(a): correlation times obtained from $\langle P_l(\mathbf{u}(0).\mathbf{u}(t)) \rangle$; (b): correlation times obtained from $\langle P_l(u_z(0)).P_l(u_z(t)) \rangle$. The numbers between brackets are the fitted C_∞ values (see text).

dramatically for $\alpha^* = 0.075$. In this last case, τ_D is estimated to be larger than the simulation length in LS10 geometry.

We have also calculated the reorientational correlation times of the unit vector $\mathbf{u}_i(t)$ along the direction of the permanent individual dipole moment. The correlation times τ_l ($l = 1$ and 2) are obtained from a biexponential fitting procedure of the autocorrelation functions $C_l(t) = \langle P_l(\mathbf{u}_i(0).\mathbf{u}_i(t)) \rangle$ of the form:

$$\frac{C_l(t) - C_\infty}{C(0) - C_\infty} = Ae^{-t/\tau_A} + (1 - A)e^{-t/\tau_B} \tag{12}$$

and $\tau_l = A\tau_A + (1 - A)\tau_B$, $P_l(x)$ being a Legendre polynomial of order l. For an isotropic system, C_∞ should be zero. The numerical values of $\tau_l^* = \tau_l \sqrt{\varepsilon_{LJ}/m\sigma_{LJ}^2}$ and C_∞ are given in Table V. For an isotropic system, the three directions x, y and z are equivalent, and τ_l can be also obtained from $\langle P_1(u_i^z(0)).P_1(u_i^z(t))\rangle$ or $\langle P_1(u_i^x(0)).\ P_1(u_i^x(t))\rangle$ or $\langle P_1(u_i^y(0)).P_1(u_i^y(t))\rangle$, similar behaviour holds for τ_2. In Table V, a second estimate of the correlation times τ_l^* obtained from $\langle P_l(u_i^z(0)).P_l(u_i^z(t))\rangle$ is included. Differences between both determinations confirm that the system is far from isotropic when $\alpha^* = 0.075$ and the anisotropy is larger in LS10 geometry than in RF geometry. Eq. (12) has also been used to obtain the correlation time τ_μ of the autocorrelation function of the total (permanent + induced) individual dipole moment reported in Table V.

We have checked that the system remains in a fluid phase and do not undergo a fluid-solid transition for all the values of the polarizability α^*. The translational diffusion coefficient D has been calculated from i) the mean square displacement and from ii) the velocity autocorrelation function; both determinations were found to be consistent. For the three values of α^*, the mean square displacement was always at long time a continuously (linearly) increasing function of time, proving that the system is not in a solid phase, so the appearance of dipolar order at sufficiently large polarizability is purely electrostatic and does not correspond to any trapping of the system in some solid-like structure. The numerical values in reduced units of the diffusion coefficient $D^* = D\sqrt{m/\varepsilon_{LJ}\sigma_{LJ}^2}$ are given in Table V. We notice that LS10 and RF give identical results, except for the case $\alpha^* = 0.075$ where the system is not anymore isotropic, the anisotropy being larger in LS10 geometry than in RF geometry.

4. CONCLUSION

Molecular Dynamics simulations have been used to compare the static dielectric constant of the polarizable Stockmayer fluid obtained by the lattice summation technique (Ladd expansion) and the Barker-Watts reaction field method. Both methods are found to give consistent and reliable estimates of the static dielectric constant if: i) the polarizability is not too large, ii) the sample size (cutoff distance in RF geometry) is large enough

and iii) the truncation of the Ladd expansion is done at sufficiently large order (in practice LS10 seems sufficient).

A point of interest is to know if these findings will remain valid for more realistic models mimicking real fluids. No definitive answer can be given to this question without extensive comparisons of both methods. Noticing that the largest values of the dielectric constant ε_0 in the liquid phase are smaller than 200, one can expect that the reaction field and lattice summations methods should give consistent results for simulation boxes containing at least 250–350 molecules. It has been observed once again that the reaction field geometry is more sensitive to the size of the system than the lattice summation technique. In both cases, it is advised to choose a sample size leading to an averaged induced dipole independent of the sample size to obtain an estimate of the dielectric constant independent of the sample size.

Acknowledgements

We thank C. Kriebel and J. Winkelmann for several discussions. We are grateful to the Centre InterRégional Informatique de Lorraine for a generous allocation of computer time on their IBM/SP1 parallel machine.

APPENDICES

A. Neglect of self interactions

In RF geometry, a dipole can interact with its own reaction field; this interaction adds a corrective self term to the energy of the system.

In LS geometry, the physical system simulated is a very large sphere (constituted by replicas of the central cell) embedded in a dielectric medium of dielectric constant ε_{RF}. Each dipole interacts with its own images and with its own reaction field; the reaction field contribution is the only surviving self energy term when the lattice summation is done inside a sphere.

If the self interactions are taken into account, the induced dipoles are given by:

$$\mathbf{p}_i = -\sum_{j \neq i} \alpha \mathbf{T}_{ij}(\boldsymbol{\mu}_j + \mathbf{p}_j) - \alpha \mathbf{T}_{ii'}(\boldsymbol{\mu}_i + \mathbf{p}_i) \tag{13}$$

with $\mathbf{T}_{ii'}$ the electrostatic self interaction tensor:

$$\mathbf{T}_{ii'} = -\frac{1}{R_c^3}\frac{2(\varepsilon_{RF}-1)}{2\varepsilon_{RF}+1}\mathbf{1} \quad \text{RF} \tag{14}$$

$$\mathbf{T}_{ii'} = -\frac{4\pi}{3V}\frac{2(\varepsilon_{RF}-1)}{2\varepsilon_{RF}+1}\mathbf{1} \quad \text{LS} \tag{15}$$

The overall electrostatic potential energy becomes:

$$U_{\text{dip}} + U_{\text{cr}} = \frac{1}{2}\sum_i \sum_{j\neq i} (\boldsymbol{\mu}_i + \mathbf{p}_i)\mathbf{T}_{ij}(\boldsymbol{\mu}_j + \mathbf{p}_j) + \frac{1}{2}\sum_i (\boldsymbol{\mu}_i + \mathbf{p}_i)\mathbf{T}_{ii'}(\boldsymbol{\mu}_i + \mathbf{p}_i) + \frac{1}{2}\sum_i \frac{\mathbf{p}_i^2}{\alpha} \tag{16}$$

Combining Eqs. (13) and (16), one obtains:

$$U_{\text{es}} = U_{\text{es}}(\text{pair}) + U_{\text{es}}(\text{self}) = \frac{1}{2}\sum_i \sum_{j\neq i} \boldsymbol{\mu}_i \mathbf{T}_{ij}\boldsymbol{\mu}_j + \frac{1}{2}\sum_i \boldsymbol{\mu}_i \mathbf{T}_{ii'}\boldsymbol{\mu}_i \tag{17}$$

$$U_{\text{ind}} = U_{\text{ind}}(\text{pair}) + U_{\text{ind}}(\text{self}) = \frac{1}{2}\sum_i \sum_{j\neq i} \boldsymbol{\mu}_i \mathbf{T}_{ij}\mathbf{p}_j + \frac{1}{2}\sum_i \boldsymbol{\mu}_i \mathbf{T}_{ii'}\mathbf{p}_i \tag{18}$$

where U(pair) and U(self) represent total intermolecular and total self energy contributions respectively.

For the case $N = 125$, $\mu^* = 1.732$, $\alpha^* = 0.05$, in RF geometry ($\varepsilon_{RF} = \infty$), the value of the cutoff R_c^* is 2.67 (7.755 Å in real units) for $\rho^* = 0.822$ ($\sigma_{\text{LJ}} = 2.906$ Å and box edge = 15.51 Å). From these values and the order of magnitude of the induced dipole ($\approx 25\%$ of the permanent dipole), the self term corrections are estimated to be $U_{\text{es}}(\text{self})^* \approx -0.08$ and $U_{\text{ind}}(\text{self})^* \approx -0.02$; as $U_{\text{es}}(ij)^* \approx -5.6$ and $U_{\text{ind}}^* \approx -1.5$, so the neglect of the self interactions introduces an error of about 1.5% in the potential energy. The error in the individual induced dipoles introduced by the neglect of self polarization is estimated to be $\approx \alpha|\boldsymbol{\mu}_i + \mathbf{p}_i|/R_c^3|\mathbf{p}_i| \approx 1\%$. During a simulation the term U_{es} (self) is a constant and only the term U_{ind}(self) fluctuates. From a physical point of view, the self interactions are not expected to change significantly the fluctuations of **M**. To check the validity of this assumption, we have repeated the RF simulation with $N = 125$, $\mu^* = 1.732$, $\alpha^* = 0.05$ and self interactions included: the values in Table III of ε_0 (170) and $\langle \mu_{\text{tot}}^{*2} \rangle$(4.50) become equal to 168 and 4.53 respectively and the energy components U_{es}^*, U_{ind}^* and U_{LJ}^* are changed by -0.13, -0.09 and $+0.01$ respectively. As the magnitude of the self interaction contributions decreases when the system size increases, the neglect of the self interactions does not affect significantly the computation of dielectric properties of this article.

B. Fluctuation formula in RF geometry with $\varepsilon_{RF} = \infty$

Following Pollock *et al.* [30], the static dielectric constant ε_0 of a system of N point dipoles $\boldsymbol{\mu}_i$ with point polarizability α is defined from the linear response of the polarization density to the macroscopic electric field $\mathbf{E}$ in the sample and given by the equation:

$$\frac{\varepsilon_0 - 1}{4\pi}\mathbf{I}\cdot\mathbf{E} = \frac{N}{3VkT}\frac{\langle \mathbf{M}^2 \rangle}{N}\mathbf{I}\cdot\mathbf{E}_{\text{ext}} + \rho\frac{\langle \mathbf{A} \rangle}{N}\cdot\mathbf{E}_{\text{ext}} \tag{19}$$

with $\mathbf{M}$ the sum of all permanent and induced dipoles in the system. $\mathbf{I}$ is the $3N \times 3N$ identity matrix and

$$\mathbf{A} = \frac{\alpha\mathbf{I}}{\mathbf{I} + \alpha\mathbf{T}} \tag{20}$$

where α is the polarizability and $\mathbf{T}$ a $3N \times 3N$ matrix containing the electrostatic tensors $\mathbf{T}_{ij}$. The relationship between $\mathbf{E}$ and $\mathbf{E}_{\text{ext}}$ depends on the shape of the sample and boundary conditions. In RF geometry with $\varepsilon_{RF} = \infty$, $\mathbf{E} = \mathbf{E}_{\text{ext}}$ and from the definition of $\mathbf{T}_{ij}$ in Eq.(4), one obtains:

$$\langle \sum_j \mathbf{T}_{ij} \rangle = -N\left(x_s \cdot \frac{1}{R_c^3} + (1 - x_s).0 \right)\mathbf{1} = -\frac{4\pi}{3}\frac{N}{V}\mathbf{1} \tag{21}$$

with x_s the fraction of particles inside the sphere of radius R_c centered on particle i. Expansion of matrix $\mathbf{A}$ leads to

$$\sum_j \langle \mathbf{A}_{ij} \rangle = \frac{\alpha\mathbf{1}}{\mathbf{1} + \alpha\langle \sum_j \mathbf{T}_{ij} \rangle} \tag{22}$$

Using the Clausius-Mossotti relationship to link α and ε_∞ and Eqs. (20)–(22), we obtain,

$$\langle \mathbf{A} \rangle = \frac{3V}{4\pi N}\left(\frac{\varepsilon_\infty - 1}{3} \right)\mathbf{I} \tag{23}$$

Eqs. (23) and (19) lead to the fluctuation formula of Eq. (6) after elimination of $\mathbf{I}\cdot\mathbf{E}_{\text{ext}}$.

In Ladd summation with $\varepsilon_{RF} = \infty$, the tensors $\mathbf{T}_4, \mathbf{T}_6, \ldots$ have zero averages as well as the direct dipole-dipole tensor and:

$$\left\langle \sum_j \mathbf{T}_{ij} \right\rangle = -\frac{4\pi N}{3V}\mathbf{1} \tag{24}$$

In that case, $\mathbf{E} = \mathbf{E}_{ext}$, and as Eq. (24) is the same as in RF geometry with $\varepsilon_{RF} = \infty$, the same fluctuation formula is obtained.

References

[1] Wertheim, M. S. (1973). "Dielectric constant of non-polar fluids", *Mol. Phys.*, **25**, 211.
[2] Wertheim, M. S. (1973). "Theory of polar fluids. I", *Mol. Phys.*, **26**, 1425.
[3] Wertheim, M. S. (1977). "Theory of polar fluids. III", *Mol. Phys.*, **34**, 1109.
[4] Patey, G. N., Levesque, D. and Weis, J. J (1982). "On the theory and computer simulation of dipolar fluids", *Mol. Phys.*, **45**, 733.
[5] Carnie, S. L. and Patey, G. N. (1982). "Fluids of polarizable hard spheres with dipoles and tetrahe dral quadrupoles. Integral equation results with application to liquid water", *Mol. Phys.*, **47**, 1129.
[6] Perkyns, J. S., Fries, P. H. and Patey, G. N. (1986). "The solution of the reference hypernetted-chain approximation for fluids of hard spheres with dipoles and quadrupoles", *Mol. Phys.*, **57**, 529.
[7] De Leeuw, S. W., Perram, J. W. and Smith, E. R. (1986). "Computer simulation of the static dielectric constant of systems with permanent electric dipoles", *Ann. Rev. Phys. Chem.*, **37**, 245.
[8] Adams, D. J. and McDonald, I. R. (1976). "Thermodynamic and dielectric properties of polar lattices", *Mol. Phys.*, **32**, 931.
[9] Pollock, E. L. and Alder, B. J. (1980). "Static dielectric properties of Stockmayer fluids", *Physica A*, **120**, 1.
[10] Neumann, M. (1987). "Dielectric properties and the convergence of multipolar lattice sums", *Mol. Phys.*, **60**, 225.
[11] Kusalik, P. G. (1992). "Determination of the transient polarization of a dipolar fluid", *Mol. Phys.*, **76**, 337.
[12] Kusalik, P. G. (1990). "Computer simulation results for the dielectric properties of a highly polar fluid", *J. Chem. Phys.*, **93**, 3520.
[13] Kusalik, P. G. (1993). "The distribution of fluctuations of the total dipole moment in polar fluids", *Mol. Phys.*, **80**, 225.
[14] Kusalik, P. G., Mandy, M. E. and Svishchev, I. M. (1994). "The dielectric constant of polar fluids and the distribution of the total dipole moment", *J. Chem. Phys.*, **100**, 7654.
[15] Neumann, M. (1985). "The dielectric constant of water. Computer simulation with the MCY potential", *J. Chem. Phys.*, **82**, 5663.
[16] Neumann, M. (1986). "Dielectric relaxation in water. Computer simulation with the TIP4P potential", *J. Chem. Phys.*, **85**, 1567.
[17] Alper, H. E. and Levy, R. M. (1989). "Computer simulation of the dielectric properties of water: studies of the simple point charge and transferable intermolecular potential models", *J. Chem. Phys.*, **91**, 1242.
[18] Ni, X. and Fine, R. M., (1992). "Determination of the dielectric constant of the water model TIP4P by free energy perturbation and induced polarization", *J. Phys. Chem.*, **96**, 2718.
[19] Kurtovic, Z., Marchi, M. and Chandler, D. (1993). "Umbrella sampling molecular dynamics study of the dielectric constant of water", *Mol. Phys.*, **78**, 1155.

[20] Goldman, S., Joslin, C. and Wasserman, E. A. (1994). "Theoretical calculation of the static dielectric constant of water at high temperatures and pressures", *J. Phys. Chem.*, **98**, 6231.
[21] Smith, P. E. and van Gunsteren, W. F. (1994). "Consistent dielectric properties of the simple point charge and extended simple point charge water models at 277 and 300 K", *J. Chem. Phys.*, **100**, 3169.
[22] Neumann, M. and Steinhauser, O. (1980). "The influence of boundary conditions used in machine simulations on the structure of polar systems", *Mol. Phys.*, **39**, 437.
[23] Neumann, M. (1983). "Dipole moment fluctuation formulas in computer simulation of polar systems", *Mol. Phys.*, **50**, 841.
[24] Neumann, M., Steinhauser, O. and Pawley, G. S. (1984). "Consistent calculation of the static and frequency-dependent dielectric constant in computer simulation", *Mol. Phys.*, **52**, 97.
[25] Neumann, M. (1986). "Computer simulation and the dielectric constant at finite wavelength", *Mol. Phys.*, **57**, 97.
[26] Smith, E. R. and Wielopolski, P. A. (1987). "Dielectric constants from computer simulations. Periodic boundary conditions, sample size and behaviour of $\varepsilon(k)$", *Mol. Phys.*, **61**, 1063.
[27] Gray, C. G., Sainger, Y. S., Joslin, C. G., Cummings, P. T. and Goldman, S. (1986). "Computer simulation of dipolar fluids. Dependence of the dielectric constant on system size: A comparative study of Ewald sum and reaction field approaches", *J. Chem. Phys.*, **85**, 1502.
[28] Ladd, A. J. C. (1977). "Monte Carlo simulation of water", *Mol. Phys.*, **33**, 1039.
[29] Ladd, A. J. C. (1978). "Long-range dipolar interactions in computer simulations of polar liquids", *Mol. Phys.*, **36**, 463.
[30] Pollock, E. L., Alder, B. J. and Patey, G. (1981). "Static dielectric properties of polarizable Stockmayer fluids", *Physica*, **108A**, 14.
[31] Mooij, G. C. A. M., De Leeuw, S. W., Smit, B. and Williams, C. P. (1992). "Molecular dynamics studies of polar/nonpolar fluid mixtures. II. Mixtures of Stockmayer and polarizable Lennard-Jones fluids", *J. Chem. Phys.*, **97**, 5113.
[32] Sprik, M. (1991). "Hydrogen bonding and the static dielectric constant in liquid water", *J. Chem. Phys.*, **95**, 6762.
[33] Zhu, S.-B., Singh, S. and Robinson, G. W. (1991). "A new flexible/polarizable water model", *J. Chem. Phys.*, **95**, 2791.
[34] Smith, D. E. and Dang, L. X. (1994). "Computer simulation of NaCl association in polarizable water", *J. Chem. Phys.*, **100**, 2791.
[35] Brodholdt, J., Sampoli, M. and Vallauri, R. (1995). "Parametrizing a polarizable intermolecular potential for water", *Mol. Phys.*, **86**, 149.
[36] Barker, J. A. and Watts, R. O. (1973). "Monte Carlo studies of the dielectric properties of water-like models", *Mol. Phys.*, **26**, 789.
[37] Vesely, F. J. (1977). "N-particle dynamics of polarizable Stockmayer-type molecules", *J. Comp. Phys.*, **24**, 361.
[38] Allen, M. P. and Tildesley, D. J. (1987). "Computer Simulations of Liquids", Clarendon, Oxford.
[39] Kriebel, C. and Winkelmann, J. (1996) "Thermodynamic properties of polarizable Stockmayer fluids: perturbation theory and simulation", *Mol. Phys.*, **88**, 559.
[40] Wei. D. and Patey, G. N. (1992). "Orientational order in simple dipolar liquids: computer simulation of a ferroelectric nematic phase", *Phys. Rev. Lett.*, **68**, 2043.
[41] Eppenga, R. and Frenkel, D. (1984). "Monte Carlo study of the isotropic and nematic phases of infinitely thin hard platelets", *Mol. Phys.*, **52**, 1303.